Combustion dynamics in a diabatic PSR with global, reduced and detailed reaction mechanisms

F.S. Marra[1], L. Acampora[1]

1. Istituto di Ricerche sulla Combustione - C.N.R., Napoli - Italy

Introduction

Combustion phenomena, especially in industrial applications, very often involve an unsteady behavior, being really transient (f.i. ignition, accidental explosions) or because affected by unsteady phenomena (f.i. noise, turbulence). The role of a selected reaction mechanism in the correct prediction of combustion dynamics is, therefore, important. Reduced chemical schemes are required for CFD simulations of reactive industrial flows. Usually, the reduction of the reaction mechanism is performed ensuring that the reduced scheme reproduces global parameters like the adiabatic temperature, the global burning rate or the laminar flame speed, rarely with an assessment of the ability to reproduce dynamical properties too [1,2].
In [3], the role of the reaction mechanism in determining the ability of a methane-air mixture to withstand forced perturbations in conditions close to extinction in an adiabatic PSR was investigated. Several issues were highlighted about the ability of global reactions to reproduce the behavior obtained with the well-established GriMech 3.0 (GRI) scheme [4].
In this work a diabatic PSR model is assumed. The previous study is extended to include a characterization of spontaneous oscillations, that can arise when a heat loss term is introduced. The bifurcation diagrams with the different mechanisms are preliminary determined. Then, simulations are performed in key solution points where periodic solutions establish, spontaneously or by a forcing. Comparison of results allows to highlight several features of system dynamic response and their dependences upon the selected mechanism.

Model Description and Methodologies

Perfectly Stirred Reactor. The equations of time evolving diabatic PSR can be written as [5]:

$$\frac{dY_j}{dt} = Y_{j,f} - \frac{Y_j}{\tau} + \frac{W_j r_j}{\rho V}, \qquad j = 1, 2, \dots, N_s$$

$$\frac{dT}{dt} = \frac{\sum_{j=1}^{N_s} Y_{j,f}\left(h_{j,f} - h_j\right)}{c_p \tau} - \frac{\sum_{j=1}^{N_s} h_j W_j r_j}{c_p \rho V} - \alpha S \frac{T - T_{env}}{c_p \rho V}$$

Here t, Y_j, τ, W_j, r_j, ρ, V, N_s, T, h, c_p, α, S refer to time, mass fraction of specie j, residence time, molecular weight of species j, molar reaction rate of species j, density, reactor volume, number of species, temperature, specific enthalpy, constant pressure specific heat, heat loss coefficient and surface area of the reactor respectively. The subscript f refers to reactor feeding (inlet) conditions and env to the environmental conditions. The residence time τ is defined as $\tau = (\rho V)/\dot{m}_f$ where $\dot{m}$ is the mass flow rate.
Chemical models. This work reports on methane-air combustion (air composition: O_2 21%, N_2 79% by volume). We will make use of a detailed kinetic schemes, a reduced mechanism and two different global reaction mechanisms.
The detailed GRI mechanism [4] is the most widely known chemical kinetics mechanism used for modelling methane and natural gas combustion in air. The current version (version 3.0) consists of 325 chemical reactions and 53 species.
The Lu and Law (LL) reduced mechanism [6] is obtained from GRI by eliminating the unimportant species and reactions applying the directed relation graph method [7]. The

corresponding author: Francesco Saverio Marra

current version consists of 184 chemical reactions and 30 species.
The 2S-CM2 mechanism [8] is a two steps global reaction mechanism tuned to reproduce GRI flame speeds for various equivalence ratios, particularly, for mixture with $T = 300$ K, pressure $p = 0.1$ MPa and equivalence ratios between 0.6 and 1.0. The reactions and full specification of Arrhenius parameters are reported in table 1 (A, β, and E_a refer respectively to pre-exponential factor, temperature exponent, and Activation Energy).

Tag	Reactions	A	β	E_a	Reaction Orders
2S-CM2-1	$CH_4 + 1.5\ O_2 \rightarrow CO + 2\ H_2O$	2×10^{15}	0	35000	$[CH_4]^{0.9}\ [O_2]^{1.1}$
2S-CM2-2	$CO + 0.5\ O_2 \rightarrow CO_2$	2×10^{9}	0	12000	$[CO]\ [O_2]^{0.5}$
2S-CM2-2r	$CO_2 \rightarrow CO + 0.5\ O^2$	8.1104×10^{10}	0	77194	$[CO_2]$

Table 1. Reactions and Arrhenius parameters for 2S-CM2 mechanism [8], (cgs units)

The Westbrook and Dryer (WD) mechanism reported as set 3 in the original work [9] was selected global one step mechanism. This set shows good (but not best) agreement between detailed mechanism and one-step mechanism but avoid negative reaction order. The reaction and full specification of Arrhenius parameters are reported in table 2.

Tag	Reactions	A	β	E_a	Reaction Orders
WD	$CH_4 + 2\ O_2 \rightarrow CO_2 + 2\ H_2O$	6.7×10^{12}	0	48400	$[CH_4]^{0.2}\ [O_2]^{1.3}$

Table 2. Reaction and Arrhenius parameters for WD mechanism [9], (cgs units)

Results and Discussion

Bifurcation map. In this work only the residence time is considered as continuation parameter. To construct the bifurcation diagram and identify the bifurcation points we use the tool described in [10]. The results for all the 4 mechanisms are shown in Fig. 1.

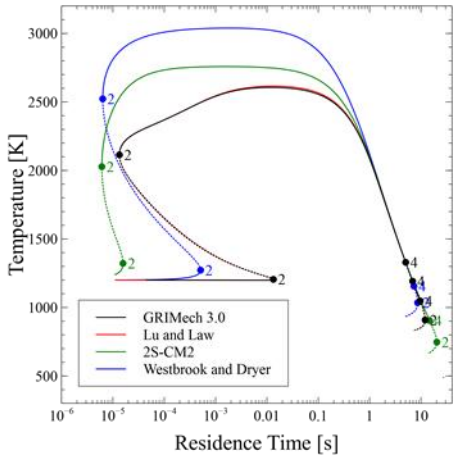

Fig. 1 Bifurcation diagram for the different reaction mechanisms

Conditions adopted are: stoichiometric mixture, atmospheric pressure and inlet temperature fixed to 1200 K. Heat transfer to the wall depends on $T_{env} = 300$ K and on the coefficient $\alpha A/V = 125.4$ W m^{-3} K^{-1}. Bifurcation points are indicated by a circle symbol and labelled with "2" if limit points and with "4" if Hopf Bifurcations. Dotted lines indicate unstable branches. Ignition of the mixture, the first limit point encountered walking the curves from the lower values of τ, occurs at very different residence times, indicating the need to adopt the GRI or the LL mechanisms if ignition phenomena are investigated. Similarly, large differences are observed in the location of the second limit point, that identifies the extinction condition at low τ. The branches of ignited solutions start from these different locations and

are completely separated up to a residence time of about 1 s. The large temperature differences depend on the different heat of reaction and the different number of species and final composition that lead to a different global specific heat. Thereafter, for higher residence times, heat losses come into play, becoming the dominant phenomenon leading to the cooling of the mixture and eventually to extinction. However, approaching this second critical condition, different behaviors manifests: before extinction, a second branch of periodic solutions arise starting from the Hopf Bifurcations only with the GRI and LL mechanisms.
The behavior of the reactor under spontaneous dynamic conditions is illustrated in Fig. 2. Simulations have been performed starting from initial conditions corresponding to the last Hopf Bifurcation of each mechanism. The residence times correspond to a shift of 0.01 s (solid lines) and 0.1 s (dashed lines) from these Bifurcation points.

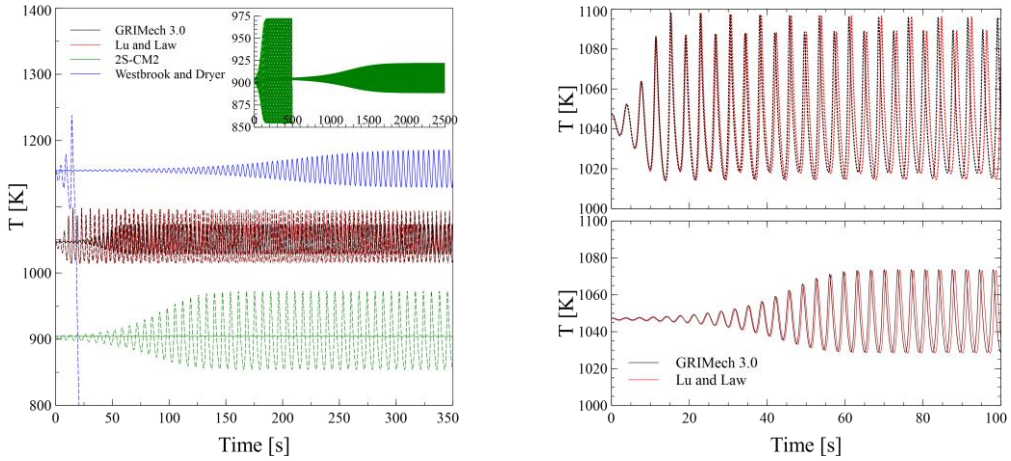

Fig. 2 Temperature vs time for the different reaction mechanisms starting from steady conditions. All mechanisms compared on the left, only GRI and LL on the right.

Noticeably, all mechanisms exhibit oscillations having frequency of the same order of magnitude, despite the different characteristic chemical time. Therefore, the oscillations are governed by a different characteristic time to be linked to the heat losses. The different dynamic emerges in the time required to reach periodic conditions and in the shape of the resulting oscillations. GRI and LL shows a period doubling moving from $\tau_{HB} + 0.01$ s to $\tau_{HB} + 0.1$ s. The development of spontaneous periodic oscillations by the application of a disturbance in steady conditions could even be not recognized if, depending on the mechanism adopted, the simulation is not advanced long enough in time. Even if the LL reduced mechanism performs very well in reproducing the behavior of the GRI, some differences arises when looking at the frequencies, leading to a time lag between the two time signals.
A different dynamic behavior is detected in steady conditions by applying a periodic forcing. A sinusoidal residence time $\tau(t) = \tau_0[1 + \varepsilon \sin(2\pi f t)]$ is imposed to the inlet conditions of the PSR. The analysis is conducted at $\tau_0 = 0.001$ s and frequency of 1000 Hz with a perturbation amplitude of 10%. Fig. 3 reports the orbits obtained compared with the baselines of the steady solution branches (dash-dot lines). Both quantitative and qualitative differences arise. Oscillations with the detailed mechanisms (GRI and LL) have a much greater amplitude. Furthermore, the slope of the main axis of the orbit is smaller than the slope of the tangent to the baseline bifurcation diagram in τ_0 for the GRI and LL mechanisms while it is greater for the reduced mechanisms. This can be explained by examining the phase shift between the temperature and methane mass fraction time signals. While T_{max} anticipate $Y_{CH_4,min}$ for the global mechanisms (only WD is shown for the sake of clarity), the contrary occurs for the detailed and reduced mechanisms (only GRI shown).

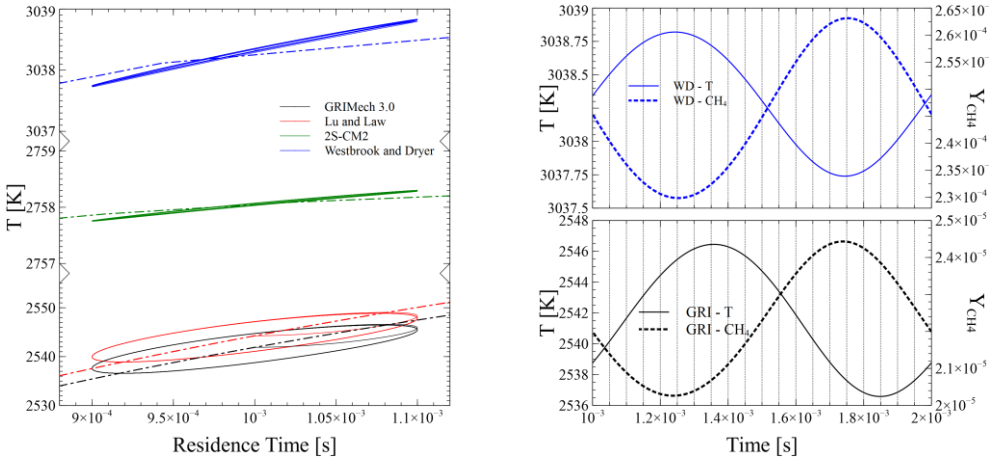

Fig. 3 Left: temperature orbits for the different reaction mechanisms starting from steady conditions. Right: temperature and methane mass fraction time signals.

Conclusions

A comparison of the dynamic features of different chemical mechanisms for the methane combustion leads to several conclusions: macroscopic, well-known, differences arise in the bifurcation diagram in regions where chemical kinetics is predominant with respect to heat losses; spontaneous periodic oscillations are reached in a longer time with the global mechanisms when shifting the residence time; periodic forcing of steady solutions leads to oscillations with different properties. The proposed analysis can contribute to a better validation of reduced schemes aiming to the simulation of dynamic combustion phenomena.

References

[1] H. S. Sidhu, L. K. Forbes, and B. F. Gray, “Forced reaction in a cstr. a comparison between the full system and the reduced model”, Chem. Eng. Sci., 52, 2667–2676, 1997.
[2] M. Valorani and S. Paolucci, “The g-scheme: A framework for multi-scale adaptive model reduction”, J. Comp. Physics, 228, 4665–4701, 2009.
[3] L. Acampora, F. S. Marra, and E. Martelli, “Non-linear response to periodic forcing of methane-air global and detailed kinetics in continuous stirred tank reactors close to extinction conditions”, Int. J. Spray Combust. Dyn., 7, 175-208, 2015.
[4] G. P. Smith, D. M. Golden, M. Frenklach, B. Eiteener, M. Goldenberg, C. T. Bowman, R. K. Hanson, W. C. Gardiner, V. V. Lissianski, and Z. W. Qin, “GRI-Mech 3.0”, 2000.
[5] T. Wada, F. Jarmolowitz, D. Abel, and N. Peters, “An instability of diluted lean methane/air combustion: Modeling and control”, Combust. Sci. Tech, 183, 1–19, 2010.
[6] T. Lu and C. K. Law, “A criterion based on computational singular perturbation for the identification of quasi steady state species: A reduced mechanism for methane oxidation with NO chemistry”, Combust. Flame, 154, 761 – 774, 2008.
[7] T. Lu and C. K. Law, “A directed relation graph method for mechanism reduction”, Proc. Combust. Inst., 30, 1333 – 1341, 2005.
[8] J. Bibrzycki and T. Poinsot, “Reduced chemical kinetic mechanisms for methane combustion in O2/N2 and O2/CO2 atmosphere”, ECCOMET WN/CFD/10, 17, 2010.
[9] C. K. Westbrook and F. L. Dryer, “Simplified Reaction Mechanisms for the Oxidation of Hydrocarbon Fuels in Flames”, Combust. Sci. Tech., 27, 31–43, 1981.
[10] L. Acampora, F.S. Marra, “Numerical strategies for the bifurcation analysis of perfectly stirred reactors with detailed combustion mechanisms”, Comput. Chem. Eng., 85, 273-282, 2015